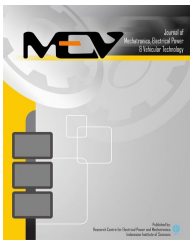

Journal of Mechatronics, Electrical Power, and Vehicular Technology 17 (2026) 1-14

Journal of Mechatronics, Electrical Power, and Vehicular Technology

e-ISSN: 2088-6985
p-ISSN: 2087-3379

mev.brin.go.id

Adaptive frequency regulation of an LPG generator using an assistive model-free iterative learning controller

Inov Ivandany [a], Arya Kusumawardana [a, *], Muhammad Afnan Habibi [b], Muhammad As'ad Sahroni [a]

[a] *Faculty of Applied Science and Technology, State University of Malang*
Semarang Street no. 5, Malang, 65145, Indonesia

[b] *School of Electronic and Electrical Engineering, University of Leeds*
Woodhouse Lane, Leeds, West Yorkshire, LS2 9JT, United Kingdom

Abstract

Mechanical speed governors in small generator sets often provide only coarse frequency regulation, leading to steady-state error and poor transient recovery under load disturbances. To address this limitation, this study proposes a hybrid governor for an (liquefied petroleum gas) LPG-converted generator, in which the built-in mechanical governor is retained as the primary stabilizing layer, and a model-free iterative learning control (ILC) is added as an assistive electronic controller. The proposed method was validated experimentally under dynamic multi-step load disturbances and internal parameter shifts. In the dynamic load test, the proposed hybrid ILC achieved the lowest root mean square error (RMSE) of 0.9144 Hz, compared with 0.9581 Hz for the (proportional-integral) PI-controller benchmark and 1.5512 Hz for the mechanical governor. This corresponds to an RMSE improvement of 41.05 % relative to the mechanical governor and 4.56 % relative to the PI-controller benchmark. In terms of relative tracking accuracy, both electronic controllers substantially reduced the mean absolute percentage error (MAPE) relative to the mechanical governor, with the proposed hybrid ILC achieving the lowest value of 1.14 %, slightly lower than 1.15 % for the PI-controller and much lower than 2.04 % for the mechanical governor. Under internal parameter detuning, the proposed method maintained better regulation performance, with RMSE improvements reaching 79.68 % relative to the mechanical baseline. These results show that the proposed hybrid model-free ILC improves transient response, tracking accuracy, and robustness, while preserving the original mechanical governor as a practical baseline controller.

Keywords: electric governor; frequency stabilization; iterative learning control (ILC); LPG-converted generator.

I. Introduction

Frequency stability is critical for secure and reliable power system operation because large and sustained deviations from the nominal frequency indicate an imbalance between generation and load demand [1]. If these deviations are not properly compensated, they can disrupt normal operation and reduce the lifetime of connected electrical equipment. Therefore, system reliability depends on whether the internal control mechanisms can effectively damp frequency fluctuations and bring the system back to a stable operating point [2][3][4].

However, mechanical governors have inherent limitations in accuracy and flexibility, which makes it difficult for them to meet modern regulation needs

* Corresponding Author. arya.kusumawardana.ft@um.ac.id (A. Kusumawardana)

https://doi.org/10.55981/j.mev.2026.1372

Received 9 February 2026; received 27 February 2026; accepted 30 March 2026; available online 19 June 2026

How to Cite: I. Ivandany *et al.*, "Adaptive frequency regulation of an LPG generator using an assistive model-free iterative learning controller," *Journal of Mechatronics, Electrical Power, and Vehicular Technology*, vol. 17, no. 1, pp. 1-14, July, 2026.

without careful tuning [5]. Their performance may degrade due to nonlinear effects and practical issues such as friction, saturation, and vibration, which often require high-precision calibration [6]. The challenge becomes more severe in low-inertia grids and systems with a high share of flexible generation, where frequency and voltage are more sensitive to disturbances. In multi-area interconnected systems, coordinated regulation of frequency and voltage is often needed rather than treating them separately [7]. For these reasons, mechanical governors may still be useful, but they often require additional support to operate reliably in complex and time-varying conditions [5][8][9].

This limitation is especially important for LPG-converted generator sets, where mechanical governors commonly provide only coarse regulation and may cause large frequency deviations when the load changes, making stability highly dependent on parameter settings [10]. Frequency stability can also worsen in systems exposed to forced oscillations, where incorrect parameters may introduce persistent distu rbances and require improved tuning strategies [11]. Furthermore, modern power systems increasingly involve power-electronic converters and non-synchronous sources, which adds complexity and motivates more intelligent control schemes [12]. To improve load–frequency regulation, robust nonlinear regulators and computer-assisted approaches have been proposed and have shown benefits such as reduced overshoot and faster responses in certain conditions [13][14][15][16]. Nevertheless, many advanced methods still rely on accurate models or extensive tuning, which can be impractical for low-cost gensets and field deployment.

To address these constraints, this paper proposes a hybrid control scheme that keeps the conventional mechanical governor as the primary (coarse) controller, while adding an electronic controller as an assistive (fine) regulator. The proposed assistive controller is based on model-free iterative learning control (ILC), following the approach described by Zhicheng Kou *et al*. [17]. The key idea is to improve regulation performance using measured operational data rather than relying on a detailed plant model, which is attractive for practical systems with uncertainty and parameter drift. Model-free control concepts have also been reported in related actuation and energy-conversion studies, supporting their practicality in real systems [18]. In addition, hybrid intelligent control ideas have been explored to improve the regulation of important system states in several applications, including power system regulation in highly variable operating conditions [19][20][21][22].

The main contribution of this work is the development and analysis of an ILC-based assistive controller aimed at consistent frequency regulation and adaptive operation in a practical generator system. ILC updates the control input iteratively using tracking errors from previous cycles, making it suitable for repetitive operating patterns where performance can improve over iterations [23]. In low-inertia environments, ILC has been discussed as a data-driven way to enhance frequency stability by effectively adding damping and inertia-like behavior [24]. Robust ILC designs, including data-driven adaptive decomposition and frequency-domain formulations, have also been proposed to support convergence when system dynamics are uncertain [25]. Nonparametric frequency-response-based ILC can further improve adaptability when task duration or operating conditions vary [26], and scheduled sliding-mode ILC has been studied to reduce sensitivity to disturbances and model uncertainty [27]. These developments highlight the potential of ILC-based methods for adaptive frequency regulation in small-scale and uncertain power-system environments [28].

II. Materials and Methods

A. Hybrid governor architecture

To improve frequency stability in the LPG-converted generator, this study proposes a hybrid governor architecture. Instead of replacing the built-in mechanical governor, we add an electronic assistive loop to enhance regulation performance. The overall idea is shown in Figure 1, and the hardware integration on the test generator is shown in Figure 2.

Figure 1 outlines how the regulation works. The measured output frequency f is used as the feedback signal, and the throttle opening is the control input that sets engine speed and, in turn, generator frequency. In this hybrid setup, the mechanical governor keeps the system stable during large and sudden load changes. At the same time, the electronic controller produces a small auxiliary correction based on the frequency deviation and sends it to the servo. This servo action makes fine adjustments to the throttle linkage, helping reduce remaining oscillations and steady-state frequency offset while keeping the original governor mechanism intact.

Figure 2 shows the implemented prototype. The servo motor is mounted near the throttle mechanism and connected through a cable/wire linkage so it can apply small corrective movements to the throttle lever. The mechanical governor assembly remains in place and continues to provide the baseline droop response.

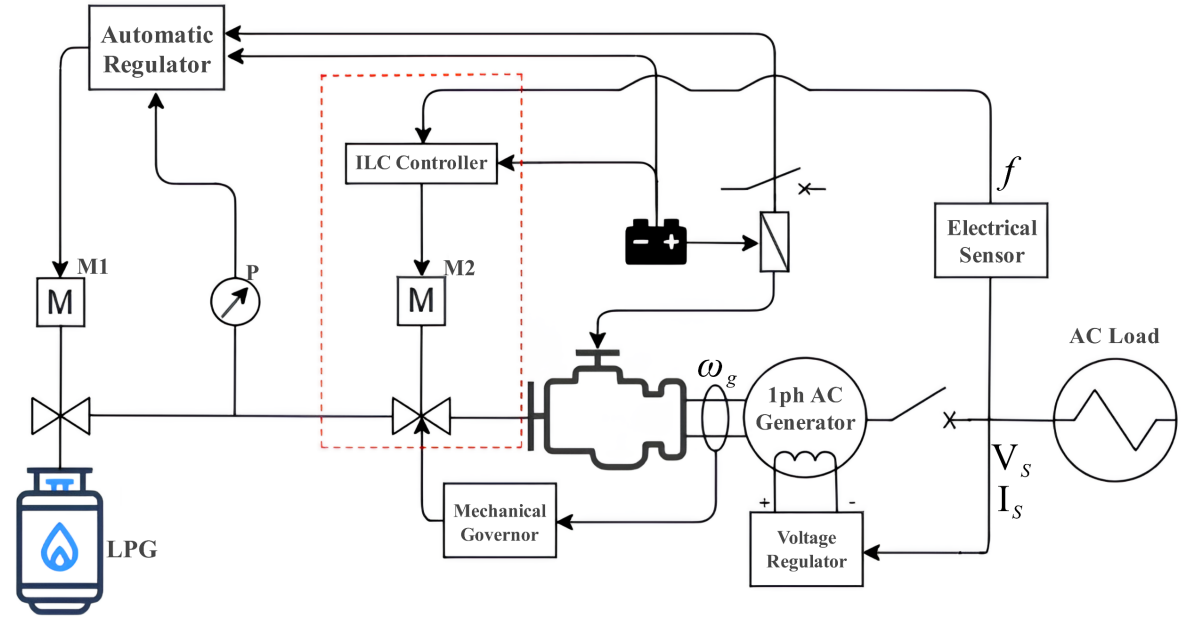

Figure 1. LPG-converted generator process diagram and proposed hybrid frequency regulation scheme.

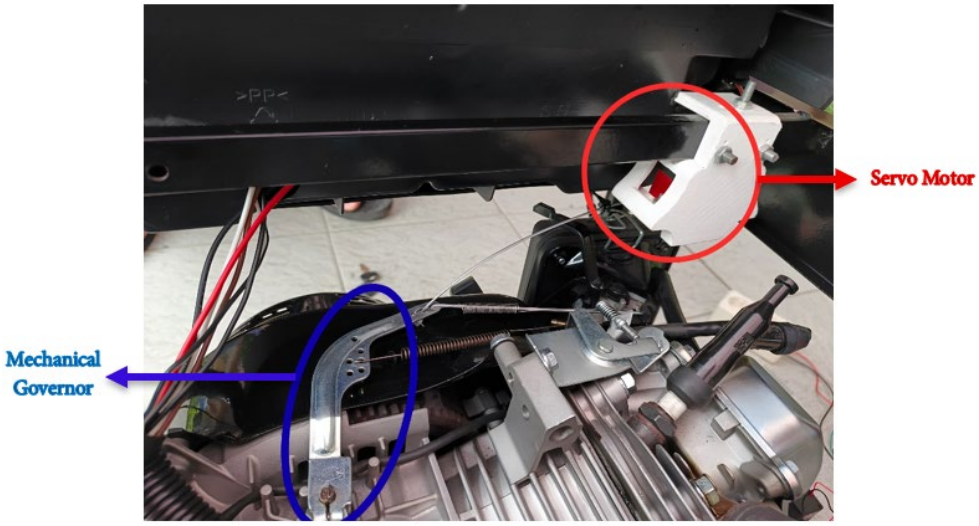

Figure 2. Implementation of hybrid governors.

With this arrangement, the servo acts as a simple add-on that improves fine regulation, while the mechanical governor still works as a robust and fail-safe baseline if the electronic loop is unavailable.

In this hybrid architecture, the two control layers have different roles so that the system remains robust while achieving better frequency accuracy:

1) Mechanical governor (primary/coarse controller)

The built-in mechanical governor is kept as the baseline controller to maintain stability under large and sudden load disturbances. Its main role is to prevent engine stall and overspeed by adjusting the throttle through a droop-like mechanical response. However, because tuning flexibility is limited and mechanical nonlinearities are unavoidable (e.g., friction and linkage backlash), the mechanical governor alone may leave a steady-state frequency offset and cause sustained oscillations, especially after LPG conversion. This makes precise tracking of the nominal frequency difficult [9].

2) Electronic governor (secondary/fine controller)

An ILC-based electronic governor is added in parallel as an assistive controller. It continuously measures the output frequency f and generates an auxiliary correction when the frequency deviates from the setpoint. This auxiliary command drives the servo actuator to introduce small corrective changes in the throttle linkage. In practice, the mechanical governor handles basic stabilization, while the ILC-based controller focuses on fine correction to reduce remaining oscillations and steady-state error, improving frequency tracking toward the nominal value [17][20].

B. The model-free ILC update law

The assistive governor in this work is based on iterative learning control (ILC). ILC is designed for systems that experience repetitive patterns, where the controller updates the input from one cycle to the next so that the tracking error gradually decreases [17]. This idea is attractive for generator applications because it can improve performance using measured data rather than relying heavily on an accurate model [20].

In the proposed hybrid setup, the ILC learns an auxiliary control signal that works alongside the mechanical governor. Across iterations, the learned signal is refined so that frequency deviations become smaller as the iteration index k increases.

This study uses an error-driven ILC update law because it is simple to implement and works well in practice [23]. The update rule that computes the auxiliary command for iteration $k+1$ using data from iteration k is given in equation (1) [29].

$$u_{k+1}(t) = Q(t)\left(u_k(t) + \gamma_p e_k(t+1) + \gamma_d\left(e_k(t+1) - e_k(t)\right)\right) \quad (1)$$

Equation (1) updates the auxiliary control signal from one iteration to the next based on the measured frequency error. The tracking error is defined as equation (2).

$$e_k(t) = f_{ref} - f_k(t) \quad (2)$$

where f_{ref} is the nominal frequency setpoint (50 Hz) and $f_k(t)$ is the measured frequency at iteration k. In this formulation, the proportional term $\gamma_p e_k(t+1)$ provides direct correction based on the magnitude of the error, while the derivative term $\gamma_d\left(e_k(t+1) - e_k(t)\right)$ adds damping by accounting for the change of error between consecutive samples. The expression inside equation (1) represents the updated control action before limitation, while $Q(t)$ denotes the bounded actuator command after the saturation function is applied.

The final actuator command is limited to the allowable servo range as equation (3).

$$Q(t) = \begin{cases} 0, & u_{k+1}(t) < 0 \\ u_{k+1}(t), & 0 \le u_{k+1}(t) \le 30 \\ 30, & u_{k+1}(t) > 30 \end{cases} \quad (3)$$

Equation (3) defines this bounded actuator command in piecewise form. In practice, any negative command is set to 0°, any command within the allowable servo range is passed directly, and any command above 30° is clipped to 30°. This constraint keeps the actuation physically feasible and prevents excessive motion of the throttle linkage. Because the control update is generated directly from the measured frequency error rather than from a detailed plant model, the proposed ILC law remains suitable for the LPG-converted generator, whose dynamics may vary with load, fuel characteristics, and mechanical conditions.

1) Model-free properties

In classical control design, controller tuning is often based on an explicit mathematical model of the plant (e.g., a transfer function). However, obtaining an accurate model for an LPG-converted engine–generator set is challenging due to nonlinearities, parameter variation, and uncertain operating conditions. The proposed ILC avoids this requirement by treating the system as a "black box" and improving performance using measured input–output data, namely the bounded actuator command $Q(t)$ and the resulting frequency error $e(t)$.

2) Learning components (memory)

The memory term is the foundation of ILC. Instead of generating a new control signal from scratch, the next-iteration command starts from the previous learned profile $u_k(t)$. This "carry-over" mechanism preserves improvements already achieved and allows the controller to refine the command progressively across iterations.

3) Error-driven correction component

The learning terms act as a correction mechanism that adjusts the stored command $u_k(t)$ based on the tracking error observed in the previous iteration. The proportional term $\gamma_p e_k(t+1)$ provides correction in proportion to the magnitude of the measured frequency error, enabling faster reduction of steady-state deviation. At the same time, the derivative term $\gamma_d\left(e_k(t+1) - e_k(t)\right)$ supplies anticipatory damping by reacting to the change in error between consecutive samples. In the discrete-time implementation, this combination helps reduce overshoot, suppress oscillations, and improve the overall transient behavior of the proposed assistive controller.

4) Saturation function

The saturation function defines the bounded actuator command $Q(t)$ by limiting the updated control signal to the allowable servo range 0°-30°. In practice, this means that any negative command is set to 0°, any command within the allowable range is passed directly to the servo, and any command above 30° is clipped to 30°. This constraint is introduced for practical safety, so that the servo and throttle linkage remain within their mechanical limits during operation.

C. Control algorithm implementation

To enable real-time execution on an embedded platform, the control logic is implemented in a structured and modular form. This modular design simplifies debugging and validation because each module has a clear role (data acquisition, control computation, actuation, and iteration management).

ALGORITHM 1

```
procedure MAINCONTROLPROGRAM
    FREQ_SETPOINT ← 50.0,FREQ_TOLERANCE ← 0.5
    γp ← 0.1, γd ← 0.009
    SERVO_ MIN ← 0, SERVO_MAX ← 30
    uk ← 0, ek(t) ← 0, ek(t+1) ← 0
    iteration ← 1, iteration_time ← 20000
    INITIALIZESERVO(SERVO_MIN)
    tstart ← CURRENTTIME()

    loop every 100 ms do
        if elapsed time ≥ iteration_time then
            iteration ← iteration + 1
            tstart ← CURRENTTIME()
            RESETTIMER()
        end if

        freq ← READPZEM()
        if freq ≠ null then
            uk ← CALCULATEILCCONTROL(freq, uk,
            ek(t), ek(t+1))
            UPDATESERVO(uk)
        end if
    end loop
end procedure
```

At start-up, an initialization routine sets the main parameters, including the frequency setpoint (50.0 Hz), the learning gains (γ_p, γ_d), actuator bounds (SERVO_MIN and SERVO_MAX), and initial state variables for the error and its difference. The controller then runs a periodic main loop with a fixed sampling time $T_s = 100$ ms. In each sample, the system reads the measured frequency f, computes the control update, and outputs the PWM command to the servo. In addition, a learning-cycle timer defines the ILC iteration window (20 s), implemented as 20000 ms in the timer; at the end of each window, the stored learning profile is updated and the iteration index advances from k to $k + 1$. The learning gains were selected empirically to achieve stable learning while avoiding excessive servo activity. During preliminary trials, γ_p was increased gradually from a small value until the frequency offset decreased consistently across iterations, and γ_d was then tuned to add damping during load transients. Based on these trials, the final gains were set to $\gamma_p = 0.1$ and $\gamma_d = 0.009$, because this combination produced the most stable response during the experiments—showing repeatable improvement without frequent saturation and without visible servo hunting around the setpoint.

Algorithm 2 implements the input-side hardware interface. It communicates with the PZEM-004T energy sensor via a serial protocol to acquire real-time electrical frequency f (and active power, if required). The routine also validates the received data so that only reliable frequency measurements are forwarded to the main loop.

ALGORITHM 2

```
function READPZEM()
    freq ← READ_FREQUENCY_FROM_SENSOR()
    if freq is valid AND freq > 10.0 then
        fcurrent ← freq
        Pcurrent ← READ_POWER_FROM_SENSOR()
        if Pcurrent is not valid then
            Pcurrent ← 0.0
        end if
        return fcurrent
    else
        fcurrent ← 0.0
        Pcurrent ← 0.0
        status ← "Sensor Read Error!"
        return null
    end if
end function
```

Algorithm 3 is the main computational routine that implements equation (1). It receives the latest measured frequency from Algorithm 2 and first computes the tracking error $e(t) = f_{ref} - f(t)$ relative to the nominal setpoint, followed by the error difference between consecutive samples to represent the derivative term required by the error-driven learning update. A practical dead-zone is then applied so that if the measured frequency remains within a predefined tolerance band (e.g., ±0.5 Hz around the setpoint), both the error and its difference are forced to zero. This effectively commands the actuator to "hold" its current throttle position rather than returning to a zero state, thereby maintaining the achieved stability, suppressing unnecessary corrective action, and preventing actuator hunting. Using the filtered error values, the algorithm updates the auxiliary command according to equation (1), and finally shifts the internal state variables so that the next loop uses the most recent error information and the latest command profile.

Algorithm 4 implements the piecewise saturation law that converts the updated control signal into the bounded actuator command $Q(t)$. This safety step clips the raw command produced by Algorithm 3 so it always stays within the physical bounds of the actuator (SERVO_MIN and SERVO_MAX). This avoids sending non-physical commands to the servo and helps protect the mechanical system.

ALGORITHM 3

```
function CALCULATEILCCONTROL(freq,uk,ek(t),ek(t+1))
    // Error Calculation
    ek(t) ← ek(t+1)
    ek(t+1) ← FREQ_SETPOINT – freq
    Δe ← ek(t+1) - ek(t)

    // Initialize control terms
    econtrol ← ek(t+1)
    Δecontrol ← Δe

    // Status determination and deadband
    if freq < (FREQ_SETPOINT - FREQ_TOLERANCE)
    then
        status ← "Assisting (Pulling)"
    else if freq >(FREQ_SETPOINT +
    FREQ_TOLERANCE) then
        status ← "Over-Freq (Releasing)"
    else
        status ← "Ideal (Holding)"
        econtrol ← 0.0
        Δecontrol ← 0.0
    end if

    // ILC update law
    learning_term ← γp * econtrol + γd * Δecontrol
    uk+1 ← uk + learning_term
    uk+1 ← SATURATE(uk+1, SERVO_MIN, SERVO_MAX)
    return uk+1
end function
```

Algorithm 5 is the output-side hardware interface. After the command is computed (Algorithm 3) and made safe (Algorithm 4), this routine generates the PWM signal and applies it to the servo motor. The servo then shifts the throttle lever position, which changes engine speed and helps correct the generator frequency.

ALGORITHM 4

```
function SATURATE(value, min_limit, max_limit)
    if value > max_limit then
        return max_limit
    else if value < min_limit then
        return min_limit
    else
        return value
    end if
end function
```

ALGORITHM 5

```
procedure UPDATESERVO(uk)
    θservo ← SATURATE(uk, SERVO_MIN, SERVO_MAX)
    WRITE_TO_SERVO(θservo)
end procedure
```

D. Experimental validation setup

A comprehensive experimental program was conducted to verify the practicality and performance of the proposed ILC-assisted frequency regulation. The tests were designed with two goals: (i) to compare frequency regulation performance between a baseline configuration and the proposed hybrid configuration under the same load disturbances, and (ii) to assess the controller's behavior when the plant condition changes (parameter drift). Two operating scenarios are evaluated: Scenario A (mechanical governor only) and Scenario B (hybrid system: mechanical governor + ILC assist).

Figure 3 shows the complete experimental setup used to validate the proposed ILC-assisted frequency regulation. The LPG generator set is treated as the plant, while a resistive load (3x500 W halogen lamps) is used to introduce load disturbances. The generator AC

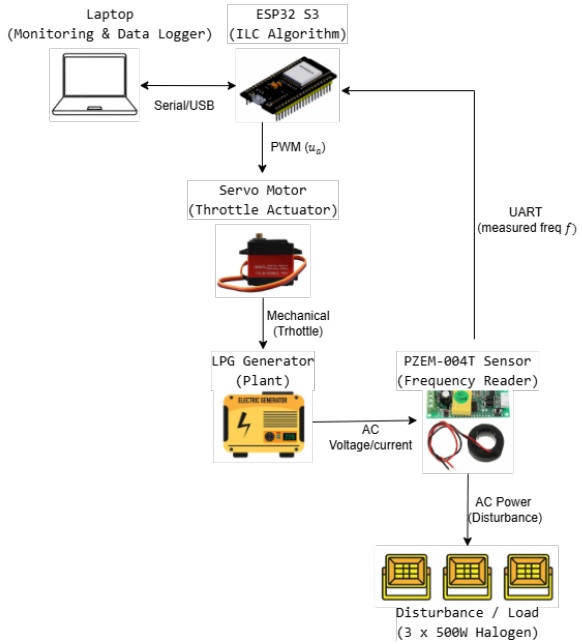

Figure 3. Block diagram of the experimental setup for ILC-assisted frequency regulation.

output is measured by the PZEM-004T module, which provides the measured frequency signal to the ESP32-S3 via UART. The ESP32-S3 runs the ILC algorithm and generates a PWM command for the servo motor. The servo then applies assistive throttle actuation through the mechanical linkage, changing engine speed and, consequently, the generator frequency. A laptop is connected via USB serial communication for monitoring and data logging during the tests.

1) Instrumentation testing and implementation platform

The experimental setup was built on a commercial generator set that was modified to operate using liquefied petroleum gas (LPG). The validation focuses on frequency regulation at the generator output under controlled step-load disturbances. The experimental control system consists of an ESP32 microcontroller, a PZEM-004T sensor, and a digital servo actuator. The ESP32 serves as the central processing unit and executes the ILC algorithm in real time with a fixed sampling time of $T_s = 100$ ms, which was selected to balance responsiveness and reliable embedded implementation. The PZEM-004T sensor is installed at the AC output of the generator to measure the actual frequency f and load power, providing the feedback signal required by the controller. Based on the measured frequency, the controller computes the corrective action and sends the bounded control command $Q(t)$, represented through the PWM interface, to the digital servo motor that is mechanically connected to the generator throttle lever. In this way, the integrated sensing, computation, and actuation chain enables the proposed assistive governor to regulate generator frequency in real time.

2) Operational scenarios and testing methodology

All testing was conducted by comparing two operational scenarios. Scenario A represents the baseline configuration, in which the system is operated only with the built-in mechanical governor to establish the reference frequency-regulation performance. Scenario B represents the hybrid configuration, in which the mechanical governor remains active as the primary coarse controller while the ILC-based electronic governor provides assistive fine-tuning. In this way, the comparison clearly distinguishes the original mechanical response from the enhanced regulation achieved by the proposed hybrid architecture.

The two main scenarios (A and B) were evaluated using two test models to assess transient response and adaptability. In addition, a conventional PI-controller was included as a benchmark only in test model 1 to provide a fair comparison under the same plant, sensor, actuator, sampling time, and load profile.

3) Test model 1: Dynamic load transient response test

This test program focuses on the comparative study of load disturbance rejection performance under the dynamic load profile. The comparison includes the baseline mechanical governor (scenario A), the proposed hybrid ILC system (scenario B), and an additional conventional PI-controller benchmark implemented under the same experimental conditions. To evaluate the performance fairly, the three control configurations were tested under the same multi-level dynamic load profile over a total duration of 200 s. In the experimental operation, one ILC iteration is defined as this 20 s time window: during the window, the controller samples the frequency at $T_s = 100$ ms and applies the auxiliary PWM command online, and at the end of the window, the measured error history is used to update the stored learning profile for the next iteration ($k \rightarrow k + 1$) according to equation (1). This window-based definition directly follows the step-load schedule in Figure 4, where each 20 s segment corresponds to one learning window. To complement the visual comparison, the dynamic load test was also evaluated using quantitative error metrics. In this study, root mean square error (RMSE) and mean absolute percentage error (MAPE) were used to quantify frequency tracking performance with respect to the 50 Hz reference. RMSE reflects the magnitude of the absolute frequency deviation, while MAPE provides a normalized measure of the average percentage tracking error [30][31]. As shown in Figure 4, this test is designed over 10 time intervals, each lasting 20 s, and consists of combined step-up and step-down loading events ranging from 0 W to 1500 W. The benchmark controller was implemented as a conventionalPI-controller using the same frequency feedback signal, actuator path, and sampling time as the proposed method.

4) Test model 2: Adaptability test for internal parameter shifts

The second test evaluates system robustness and adaptability against internal parameter changes (plant parameter drift). In this test, the calibration bolts of the mechanical governor are manually loosened in increments of -3.33 %, -6.67 %, and -10.0 % to emulate parameter drift. Under each detuned condition, a sudden 1000 W step-load is applied to the system to observe its degraded transient recovery. Finally, the responses of Scenarios A and B are compared to assess how well the proposed system adapts to changes in the plant [11]. The PI-controller benchmark was only used

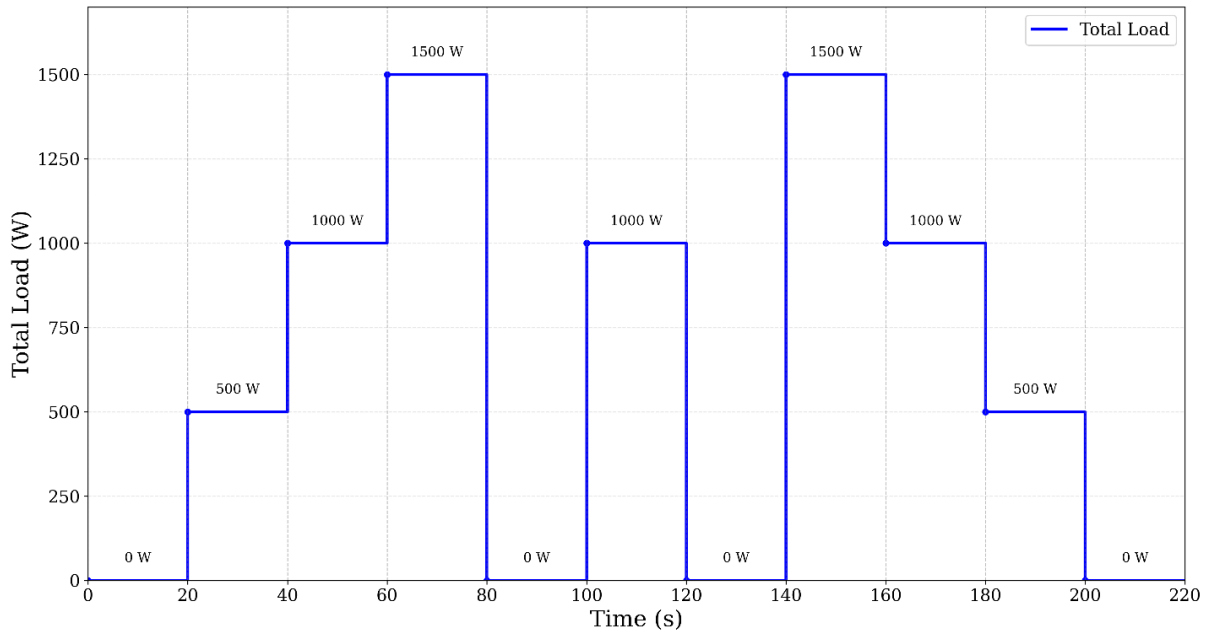

Figure 4. Multi-step dynamic load profile for system testing.

in test model 1 for dynamic load comparison and was not included in test model 2, which specifically evaluates adaptability to internal parameter shifts.

The two test models were designed to evaluate the proposed controller from two perspectives: transient performance under dynamic load variations and adaptability under internal parameter shifts. The results of these experiments are presented and discussed in the next section.

III. Results and Discussions

This section presents the experimental results and discusses the frequency regulation performance of the tested control configurations under dynamic load variations and internal parameter shifts. The analysis focuses on two main aspects: transient response during load disturbances and adaptability when the plant condition changes. To support the discussion, the results are evaluated using both response trends and quantitative performance measures, including RMSE and MAPE.

A. Analysis of dynamic load response

The dynamic load transient test was conducted to evaluate how effectively each control configuration rejects load disturbances under a time-varying load profile. In this test, three control configurations were compared under the same experimental conditions: the baseline mechanical governor, the PI-controller benchmark, and the proposed hybrid ILC system. The responses were analyzed using the multi-step load sequence defined in Figure 4, while the overall tracking performance was evaluated qualitatively from the response curves and quantitatively using RMSE and MAPE.

Figure 5 shows that the baseline mechanical governor (red line) shows clear limitations when the load changes abruptly. For example, when the load increases to 1000 W at $t = 41$ s, the frequency drops from about 48.1 Hz to 47.3 Hz and does not recover to the nominal 50 Hz value. Instead, the response remains around 47.3-47.4 Hz, indicating a persistent steady-state error. In addition, when the full load is released at $t = 81$ s, the mechanical system exhibits poor damping, with a large overshoot reaching 51.8 Hz. This behavior is consistent with the droop-based nature of a purely mechanical governor, which can provide basic stabilization but cannot fully eliminate the remaining steady-state deviation after a disturbance [9].

The PI-controller benchmark also improves regulation performance compared with the baseline mechanical governor, particularly by reducing the steady-state error and producing a more active recovery under repeated load changes. Although the PI response is clearly better than the purely mechanical governor, the overall tracking quality is still slightly inferior to that of the proposed hybrid ILC when evaluated over the full dynamic-load profile. This difference becomes more evident in the quantitative analysis presented later through the RMSE and MAPE metrics.

In contrast, the proposed hybrid ILC system shows a much-improved transient response under the same disturbance. At $t = 41$ s, the frequency undershoot is reduced significantly, with the minimum value remaining around 49.6 Hz. More importantly, the system recovers rapidly toward the nominal value

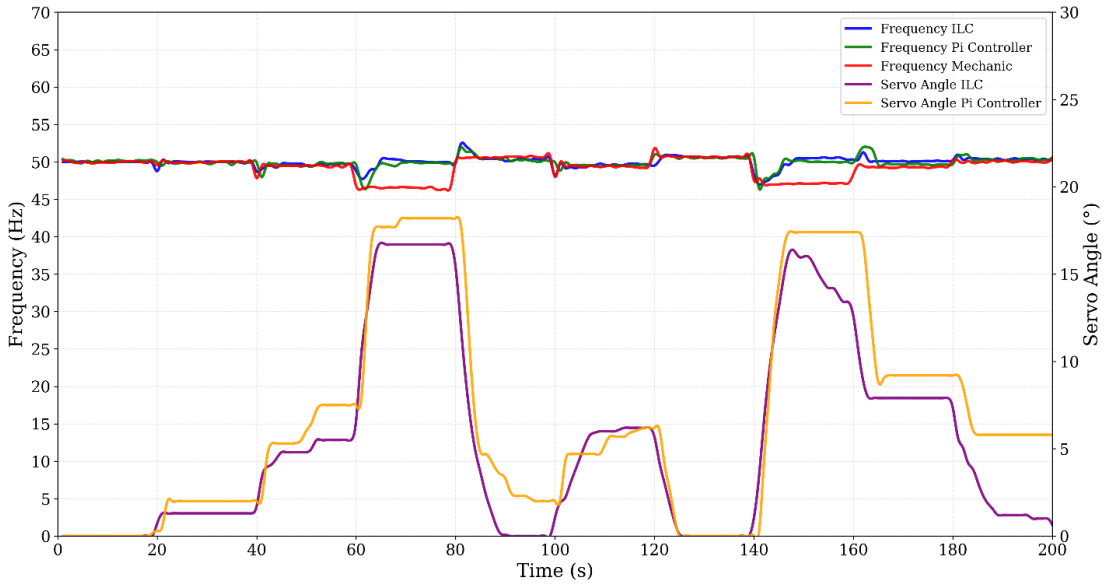

Figure 5. Comparison of frequency responses of the mechanical governor, PI-controller, and hybrid ILC during the dynamic load profile.

instead of settling at a lower steady-state level. During load release at $t = 81$ s, the overshoot is also strongly suppressed, with the maximum frequency rising only to about 50.3 Hz. These results indicate that the assistive ILC loop improves both disturbance rejection and post-transient recovery.

Compared with the PI-controller benchmark, the proposed hybrid ILC provides superior overall frequency regulation. While the conventional PI-controller relies continuously on real-time continuous error integration and is susceptible to integral windup under multi-step disturbances, the ILC refines its response by learning the recurring residual error from past cycles. This allows the hybrid system to effectively "memorize" the required throttle compensation, reducing undershoot and limiting overshoot more effectively than conventional feedback control.

This improvement can be explained by the different roles of the two control layers in the hybrid structure. The mechanical governor provides the primary stabilizing action during sudden load variations, while the ILC-based assistive controller refines the response by learning the recurring residual error and generating an additional corrective command through the servo actuator [17][20]. In this way, the hybrid system reduces undershoot, limits overshoot, and mitigates the steady-state offset more effectively than the purely mechanical governor. The observed behavior is also consistent with the error-driven nature of the proposed ILC, where the direct error term helps reduce the residual offset and the difference term contributes additional damping during transients [23].

These results provide practical evidence that the assistive ILC layer functions as intended in the proposed hybrid structure. The elimination of the steady-state offset indicates that the learned auxiliary command can compensate for the residual error left by the mechanical governor. At the same time, the reduced undershoot and overshoot show that the error-driven learning update improves transient regulation by combining direct error correction with additional damping. In this sense, the hybrid controller not only preserves the baseline stability of the mechanical governor but also enhances tracking accuracy and transient quality under repeated load changes [17][23].

From a practical perspective, this improvement is important for LPG-converted generator operation, where large frequency excursions may degrade power quality and affect connected loads. By keeping the frequency closer to the 50 Hz setpoint during both loading and unloading events, the proposed hybrid controller provides a more stable operating condition than the baseline mechanical governor. Together with the RMSE and MAPE results, this finding strengthens the conclusion that the proposed assistive ILC strategy offers better regulation quality under dynamic load disturbances.

B. Controller adaptability analysis

This test evaluates the adaptability of the proposed control strategy when the plant condition changes due to internal parameter shifts. In this study, the parameter shift is introduced by loosening the calibration bolts of the mechanical governor in several increments, namely -3.33 %, 6.67 %, and -10 %. As illustrated in Figure 6, Figure 7, and Figure 8, the detuned system initially operates at no-load, and a 1000 W step-load is suddenly applied (at $t = 10$ s, $t = 20$ s, and $t = 25$ s, respectively) to trigger the transient response.

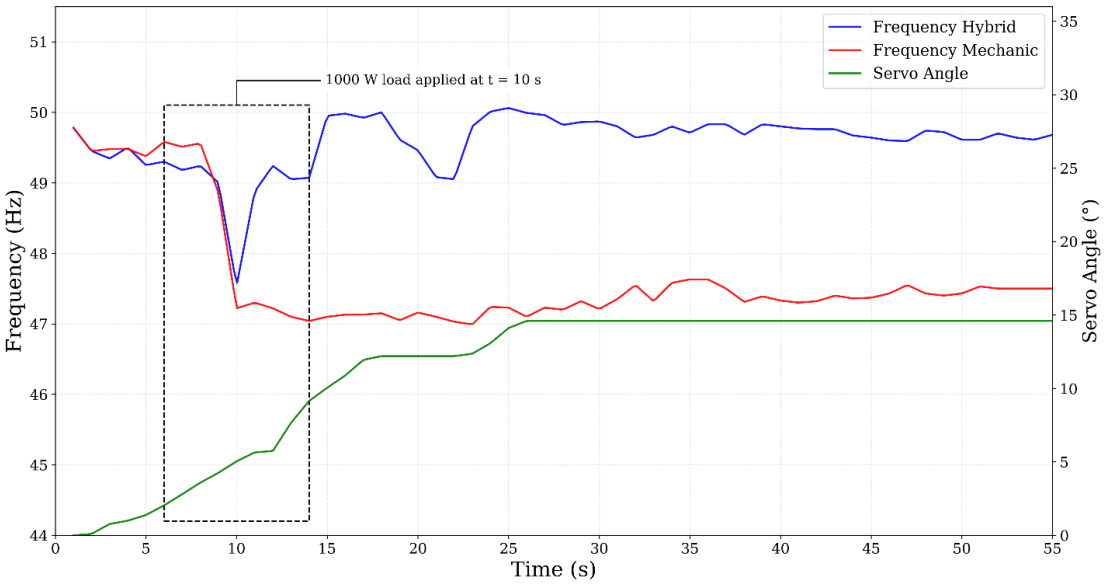

Figure 6. System response to −3.33 % detuning parameter.

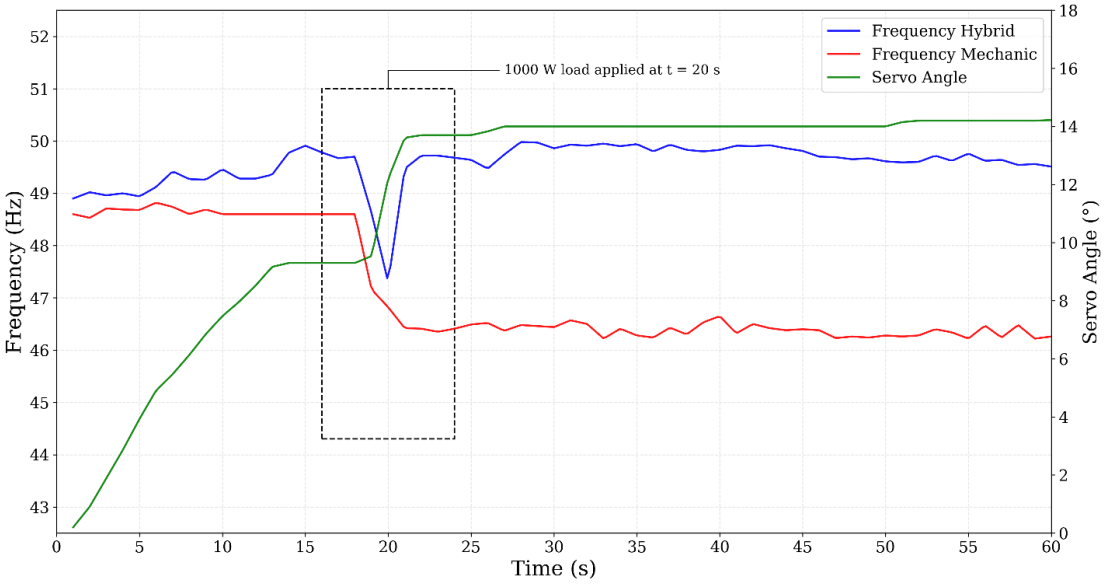

Figure 7. System response to −6.67 % detuning parameter.

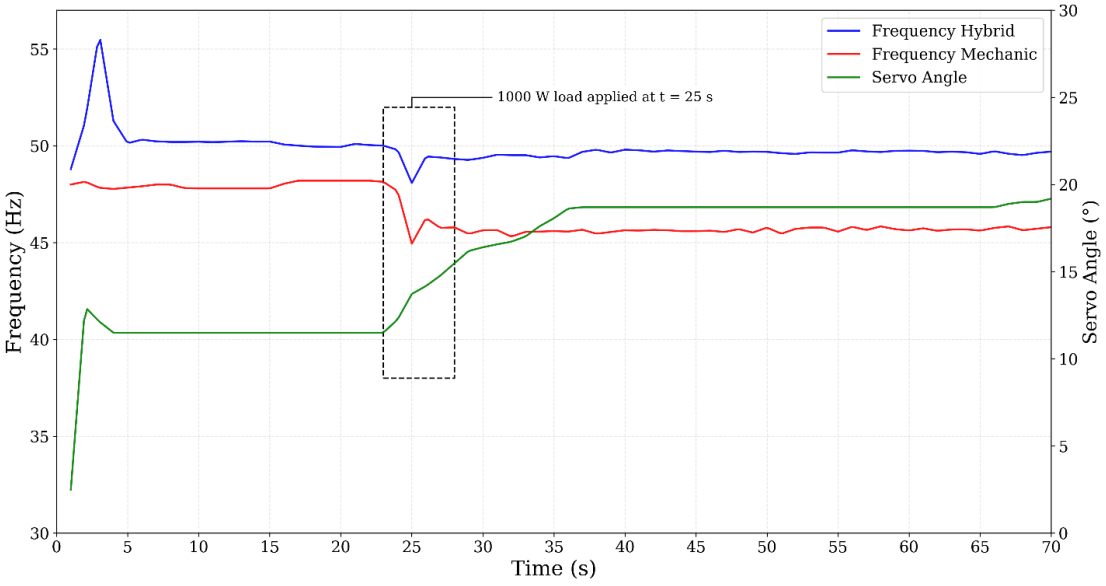

Figure 8. System response to −10 % detuning parameter.

1) Response Analysis on Detuning −3.33 %

Under the -3.33 % detuning condition, the mechanical-governor-only configuration begins to show a visible degradation in regulation quality. Although the system remains stable, the response exhibits a larger frequency deviation and a slower return toward the nominal value than in the nominal setting. This indicates that even a mild shift in the governor calibration can affect the balance between droop response and damping, leading to a less accurate frequency recovery [11].

By contrast, the proposed hybrid ILC system remains better regulated under the same detuning condition. The assistive controller continues to provide corrective throttle action based on the measured residual error, which helps maintain the frequency closer to the setpoint despite the change in plant behavior. This result suggests that the learned correction term is still effective under a moderate parameter shift, allowing the hybrid structure to preserve better tracking performance than the purely mechanical governor [17][23].

2) Response analysis on detuning −6.67 %

When the detuning level is increased to -6.67 %, the difference between the two control configurations becomes more pronounced. The baseline mechanical governor shows a stronger sensitivity to the altered parameter setting, as reflected by a larger frequency excursion and a more persistent deviation from the nominal operating point. This behavior indicates that the original mechanical regulation becomes less robust as the governor characteristics move further away from the tuned condition [11].

In comparison, the hybrid ILC system still shows a more controlled response. Although the parameter shift affects the overall plant dynamics, the assistive controller continues to reduce the residual error more effectively than the mechanical governor alone. The improvement under this condition indicates that the proposed method is not limited to a single nominal operating point, but retains a useful degree of adaptability when the plant characteristics change within a moderate range [17][20].

3) Response analysis on detuning −10 %

The -10 % detuning case represents the most severe parameter shift considered in this study and therefore provides the strongest test of controller adaptability. Under this condition, the baseline mechanical governor experiences the largest deterioration in performance, with poorer recovery characteristics and a greater tendency to remain away from the nominal frequency. This result confirms that substantial changes in governor calibration can significantly reduce the effectiveness of purely mechanical regulation [11].

The proposed hybrid ILC system also experiences performance degradation under this severe detuning condition, but it still maintains a better response than the baseline mechanical configuration. The assistive controller is able to compensate for part of the deviation by continuing to apply learned corrective action, even though the plant no longer matches the original operating condition exactly. This result shows that the proposed method improves robustness against parameter drift, although the degree of improvement naturally becomes smaller as the detuning level increases. Therefore, the adaptability test supports the claim that the hybrid ILC strategy offers better tolerance to internal parameter variations than the standalone mechanical governor [17][23].

Overall, the adaptability test shows that the proposed hybrid controller provides a more resilient frequency regulation response under internal parameter shifts than the baseline mechanical governor. As the detuning level increases, both systems experience a reduction in performance; however, the hybrid ILC structure consistently preserves better recovery and smaller residual deviation. This trend indicates that the assistive learning-based correction improves robustness against plant uncertainty and parameter drift, which is important for practical generator operation where the governor characteristics may change over time [11][17].

C. Quantitative performance evaluation (RMSE and MAPE)

To complement the visual analysis presented in the previous subsections, the controller performance was also evaluated using quantitative error metrics. In this study, root mean square error (RMSE) was used to measure the magnitude of the frequency deviation from the 50 Hz reference over the test duration. In addition, mean absolute percentage error (MAPE) was used to evaluate the relative tracking accuracy of the controllers in percentage form. Together, these two metrics provide a clearer basis for comparing the regulation quality of the tested control configurations.

Based on the Table 1, the RMSE results show that both electronic control strategies improve frequency regulation compared with the baseline mechanical governor. In the dynamic load test, the RMSE decreases from 1.5512 Hz for the mechanical governor to 0.9581 Hz for the PI-controller benchmark and to 0.9144 Hz for the proposed hybrid ILC. This corresponds to RMSE improvements of 38.23 % for the

Table 1.
Comparative RMSE results.

Test model	Test condition	Hybrid freq. RMSE (Hz)	Mechanical freq .RMSE (Hz)	Performance improvement (%)
Dynamic response	Dynamic load ILC	0.9144	1.5512	41.05 %
	Dynamic load PI-controller	0.9581	1.5512	38.23 %
Adaptability ILC	Detuning -3.33 %	0.6057	2.5260	76.02 %
	Detuning -6.67 %	0.6487	3.1916	79.68 %
	Detuning -10 %	0.9521	3.7596	74.68 %

PI-controller and 41.05 % for the hybrid ILC relative to the mechanical baseline. In direct comparison, the hybrid ILC also improves RMSE by 4.56 % relative to the PI-controller benchmark. These results indicate that both electronic control strategies reduce the absolute frequency deviation, but the proposed hybrid ILC provides the best overall RMSE performance under the dynamic load profile.

In addition to RMSE, MAPE was used to compare the relative tracking accuracy of the controllers with respect to the 50 Hz reference. Unlike RMSE, which reflects the magnitude of the absolute deviation, MAPE expresses the average tracking error in percentage form and therefore provides a normalized measure of controller performance. In this study, the MAPE comparison was used to evaluate the dynamic load test among the baseline mechanical governor, the conventional PI-controller benchmark, and the proposed hybrid ILC system [30][31].

According to Table 2, the MAPE results reinforce the same conclusion obtained from the response curves and RMSE analysis. The baseline mechanical governor records the largest average percentage tracking error, with a MAPE of 2.04 %, while the PI-controller benchmark reduces this error to 1.15 %. The proposed hybrid ILC achieves the lowest MAPE, namely 1.14 %, indicating the best overall tracking accuracy under the dynamic load profile. Relative to the mechanical governor, the PI-controller improves MAPE by 43.86 %, whereas the proposed hybrid ILC improves it by 44.01 %. Furthermore, compared with the PI-controller benchmark, the proposed hybrid ILC provides an additional 0.27 % reduction in MAPE. These results show that the proposed learning-based assistive strategy not only outperforms the baseline mechanical governor but also provides slightly more consistent tracking accuracy than the conventional PI-controller benchmark [30][31].

Table 2.
Comparative MAPE results under the dynamic load transient test.

Control configuration	MAPE (%)	Improvement relative to mechanical governor (%)
Mechanical governor	2.04	–
PI-controller	1.15	43.86
Hybrid ILC	1.14	44.01

To provide a statistical context for these results, the standard interpretation proposed by Lewis (1982) categorizes a MAPE value of less than 10 % as highly accurate [32]. Based on this criterion, the mechanical governor's baseline MAPE of 2.04 % already falls within the highly accurate category. Both electronic controllers successfully reduce this average percentage error further. The hybrid ILC achieves a relative improvement of 44.01 % over the mechanical baseline. While the absolute difference in tracking accuracy between the hybrid ILC (1.14 %) and the PI-controller (1.15 %) is marginal, the consistent error reduction from the 2.04 % baseline confirms that the assistive learning layer measurably enhances regulation precision under dynamic load variations without requiring an overly complex control structure.

The standard deviation of the measured frequency with respect to the 50 Hz setpoint provides an additional indication of response stability over the full dynamic load profile. The mechanical governor shows the largest fluctuation, with a standard deviation of 1.3862 Hz, while the PI-controller benchmark reduces this value to 0.7611 Hz. The proposed hybrid ILC achieves the smallest standard deviation, namely 0.7283 Hz, which corresponds to a 47.46 % reduction relative to the mechanical governor and a 4.32 % reduction relative to the PI-controller. This confirms that the proposed hybrid ILC maintains the frequency closer to the nominal value with less fluctuation over time.

IV. Conclusion

This study proposed and experimentally validated a hybrid governor for frequency regulation in an LPG-converted generator, in which the mechanical governor was retained as the primary stabilizing layer and a model-free ILC was used as an assistive controller. The results show that the proposed method improves both transient response and tracking accuracy under dynamic load disturbances. In the dynamic load test,

the hybrid ILC reduced RMSE by 41.05 % relative to the baseline mechanical governor and achieved the lowest MAPE of 1.14 %, compared with 1.15 % for the PI-controller benchmark and 2.04 % for the mechanical governor. Based on standard statistical interpretations, an MAPE below 10 % is classified as highly accurate. Thus, while the baseline mechanical system already operates with high accuracy, the proposed hybrid ILC further improves regulation precision by achieving a 44.01 % relative error reduction compared to the mechanical baseline, demonstrating a measurable enhancement in tracking accuracy without requiring complex parameter tuning. The adaptability test further showed that the hybrid controller maintained better regulation than the standalone mechanical governor under internal parameter shifts. Although both systems degraded as detuning increased, the hybrid ILC consistently preserved smaller frequency deviation and smoother recovery, with RMSE improvements reaching up to 79.68 % under detuned conditions. These results indicate that the proposed method improves robustness against plant uncertainty and governor drift. However, this study is still limited to resistive step-load testing and empirically tuned controller parameters. Future work should therefore examine more complex load types and adaptive tuning strategies to further improve performance under broader operating conditions. Compared with recent advanced frequency-regulation approaches in the literature, the present work emphasizes practical experimental validation of a simpler assistive learning controller for a low-cost standalone generator.

Acknowledgements

The author would like to express his deepest gratitude to the Faculty of Vocational Studies, State University of Malang, for the facilities and infrastructure provided throughout this research. Special thanks are extended to the Applied Renewable Power Electronics and Control System (ARPECS) Research Group for their technical assistance and guidance in the process of building and testing the device.

Declarations

Author contribution

I. Ivandany: Methodology (Hardware and Mechanical Design), Investigation (Test Execution), Data Curation (Data Collection), Writing – Original Draft. **A. Kusumawardana**: Conceptualization (Algorithm Design), Formal Analysis (Evaluation of Test Results), Writing – Original Draft, and Writing – Review & Editing. **M. A. Habibi:** Formal Analysis (Evaluation of System Test Results), Writing – Review & Editing. **M. A. Sahroni:** Methodology (Hardware and Mechanical Design), Investigation (Test Execution), Data Curation (Data Collection).

Funding statement

This research did not receive any specific grant from funding agencies in the public, commercial, or not-for-profit sectors.

Competing interest

The authors declare that they have no known competing financial interests or personal relationships that could have appeared to influence the work reported in this paper.

The use of AI or AI-assisted technologies

During the preparation of this work the author(s) used Gemini in order to check language clarity and grammar. After using this tool/service, the author(s) reviewed and edited the content as needed and take(s) full responsibility for the content of the publication.

Additional information

References

[1] C. Chi, H. Zhao, and J. Han, "Study on quantitative evaluation index of power system frequency response capability," *Energies*, vol. 15, no. 24, 2022.

[2] Mudakir, Aripriharta, and A. P. Wibawa, "Analysis of battery energy storage system (BESS) performance in reducing the impact of variable renewable energy generation intermittency on the electricity system," *J. Mechatronics, Electr. Power, Veh. Technol.*, vol. 15, no. 2, pp. 158–176, 2024.

[3] I. I. Novendra, I. M. Wirawan, A. Kusumawardana, and A. K. Latt, "Optimization of load frequency control using grey wolf optimizer in micro hydro power plants," *J. Mechatronics, Electr. Power, Veh. Technol.*, vol. 14, no. 2, pp. 166–176, 2023.

[4] Sujito, R. R. Hadi, L. Gumilar, A. I. Syah, M. Z. Falah, and T. H. Duy, "Long-term forecasting for growth of electricity load based on customer sectors," *J. Mechatronics, Electr. Power, Veh. Technol.*, vol. 13, no. 2, pp. 214–221, 2022.

[5] N. Nahak, J. Samal, S. K. Swain, S. Satapathy, and A. K. Patra, "Enhancement of oscillatory stability of a grid integrated microgrid by optimized governor damping

action," in *Lecture Notes in Electrical Engineering*, vol. 974, 2023, pp. 119–132.

[6] A. Big-Alabo, "On the nonlinear asymmetric vibrations of the unforced Watt governor: An exact analysis," *Adv. Mech. Eng.*, vol. 17, no. 6, Jun 2025.

[7] A. C. Barajas *et al.*, "LFC and AVR combined regulation of multi-area interconnected power system with low inertia and high penetration of flexible generation technologies," in *2023 IEEE International Autumn Meeting on Power, Electronics and Computing (ROPEC), IEEE*, Okt 2023, pp. 1–6.

[8] S. Gorb, M. Levinskyi, and M. Budurov, "Sensitivity optimisation of a main marine diesel engine electronic speed governor," *Sci. Horizons*, vol. 24, no. 11, pp. 9–19, Feb 2022.

[9] J. S. Bryant, P. Sokolowski, R. Jennings, and L. Meegahapola, "Synchronous generator governor response: performance implications under high share of inverter-based renewable energy sources," *IEEE Trans. Power Syst.*, vol. 36, no. 3, pp. 2721–2724, 2021.

[10] W. Adhyaksa, M. Anshar, and R. Tandioga, "Analisis pengaruh perubahan frekuensi sistem terhadap kinerja governor pada PLTA Bakaru Unit 1," *J. Tek. Mesin Sinergi*, vol. 23, no. 1, pp. 82–87, Sep 2025.

[11] N. L. Thotakura, C. R. Burge, and Y. Liu, "Impact of the exciter and governor parameters on forced oscillations," *Electronics*, vol. 13, no. 16, pp. 3177, Aug 2024.

[12] A. Shrestha and F. Gonzalez-Longatt, "Frequency stability issues and research opportunities in converter dominated power system," *Energies*, vol. 14, no. 14, pp. 4184, Jul 2021.

[13] V. T. Nguyen, T. L.-T. Tran, D. H. Tuan, D. C. Hien, V. P. Nguyen, and V. Van Huynh, "Load frequency control for integrated hydro and thermal power plant power system," *Int. J. Electr. Comput. Eng.*, vol. 15, no. 4, pp. 3583, Aug 2025.

[14] S. Ebrahimian, H. Shahinzadeh, H. Nafisi, M. Bagheri, M. Moazzami, and E. Etemadnia, "Enhanced frequency regulation in islanded microgrids using a machine learning-assisted linear-quadratic regulator," in *2025 6th International Conference on Optimizing Electrical Energy Consumption (OEEC), IEEE*, Feb 2025, pp. 1–7.

[15] M. Jabari, D. Izci, S. Ekinci, M. Bajaj, V. Blazek, and L. Prokop, "A novel artificial intelligence based multistage controller for load frequency control in power systems," *Sci. Rep.*, vol. 14, no. 1, pp. 29571, Nov 2024.

[16] Sasikumar K., Velmurugan K., "Optimal Frequency and Voltage Control of Self-Excited Induction Generator for Wind Power Generation Using PWM Converter and Load Management," *Int. Res. J. Mod. Eng. Technol. Sci.*, Jul., 2023.

[17] Z. Kou, J. Sun, G. Su, M. Wang, and H. Yan, "Hybrid-based model-free iterative learning control with optimal performance," *Int. J. Syst. Sci.*, vol. 54, no. 10, pp. 2268–2280, Jul 2023.

[18] M. H. Shahna and J. Mattila, "Model-free generic robust control for servo-driven actuation mechanisms with layered insight into energy conversions," *2025 American Control Conference (ACC)*, Aug., 2025.

[19] Y. Dou and E. Prempain, "Green ILC: A Novel Energy-Efficient Iterative Learning Control Approach," *Sensors*, vol. 24, no. 23, pp. 7787, Des 2024.

[20] R. Hou, L. Jia, X. Bu, and C. Peng, "Event‐triggered model‐free neuroadaptive iterative learning control via controller dynamic linearization and application to impact load frequency regulation," *Int. J. Robust Nonlinear Control*, vol. 35, no. 6, pp. 2273‐2287, Apr 2025.

[21] A. F. Mohammed, H. M. Marhoon, N. Basil, and A. Ma'arif, "A new hybrid intelligent fractional order proportional double derivative + integral (FOPDD+I) controller with ANFIS simulated on automatic voltage regulator system," *Int. J. Robot. Control Syst.*, vol. 4, no. 2, pp. 463–479, Apr 2024.

[22] M. A. El-Hameed, M. Saeed, A. Kabbani, and E. Abd El-Hay, "Efficient load frequency controller for a power system comprising renewable resources based on deep reinforcement learning," *Sci. Rep.*, vol. 15, no. 1, pp. 18379, May 2025.

[23] D. T. T. Huyen, V. Van Hoc, and N. T. T. Hoa, "Proportional derivative – type iterative learning algorithm for a motion control system," *Int. J. Robot. Control Syst.*, vol. 3, no. 2, pp. 304–314, Apr 2023.

[24] W. Y. Fu, X. D. Li, and T. Qian, "Data-driven ILC algorithms using AFD in frequency domain for unknown linear discrete-time systems," J. Franklin Inst., vol. 359, no. 6, pp. 2445–2462, 2022.

[25] W.-Y. Fu and Z. Nie, "Frequency-domain-based forgetting-factor data-driven iterative learning control algorithm," in *2024 IEEE 13th Data Driven Control and Learning Systems Conference (DDCLS), IEEE*, May 2024, pp. 878–882.

[26] V. T. Nguyen, T. B. T. Truong, Q. V. Truong, H. V. P. Nguyen, and M. Q. Duong, "Iterative learning control for virtual inertia: Improving frequency stability in renewable energy microgrids," *Sustainability*, vol. 17, no. 15, pp. 6727, Jul 2025.

[27] W.-H. Hsieh, Y.-S. Chen, and S.-T. Wu, "Iterative learning control of an inverse novel ball screw transmission system," *J. Intell. Fuzzy Syst.*, vol. 40, no. 4, pp. 8043–8052, Apr 2021.

[28] Q. Yao, H. Jahanshahi, S. Bekiros, S. F. Mihalache, and N. D. Alotaibi, "Gain-scheduled sliding-mode-type iterative learning control design for mechanical systems," *Mathematics*, vol. 10, no. 16, pp. 3005, Aug 2022.

[29] MathWorks. Iterative learning control. MATLAB Help Center. [Online].

[30] R. J. Hyndman and A. B. Koehler, "Another look at measures of forecast accuracy," *Int. J. Forecast.*, vol. 22, no. 4, pp. 679–688, 2006.

[31] A. de Myttenaere, B. Golden, B. Le Grand, and F. Rossi, "Mean absolute percentage error for regression models," *Neurocomputing*, vol. 192, pp. 38–48, 2016.

[32] C. D. Lewis. Industrial and business forecasting methods : A practical guide to exponential smoothing and curve fitting. 1982. [Online].